

Theoretical Investigation of the Electron-Correlation Effects on the Ground-State Properties of Cerium Dioxide

Elena Voloshina and Beate Paulus*

*Max-Planck-Institut für Physik komplexer Systeme,
Nöthnitzer Str. 38, D-01187 Dresden*

(Dated: October 5, 2005)

Abstract

The electron-correlation effects on the ground-state properties of CeO_2 are studied by *ab initio* quantum-chemical methods. For this purpose the method of increments, that combines the Hartree-Fock calculations for periodic systems with correlation calculations requiring only information of the corresponding finite-cluster calculations, is applied for the studied crystal. Using the coupled-cluster approach for the evaluation of the individual increments, we recover 93 % of the experimental cohesive energy. The obtained lattice constant and bulk modulus are found in good agreement with experimental values. For comparison the results obtained with density functional methods are presented.

PACS numbers: 31.15.Ar, 31.25.-v, 71.15.Nc

*Electronic address: beate@mpipks-dresden.mpg.de

I. INTRODUCTION

Ceria (CeO_2) is a technologically important material with remarkable properties used in a number of applications [1–4]. The cerium dioxide is known to exist in the cubic fluorite structure (Fig. 1), which is the stable polymorph at all temperatures [5]. CeO_2 is an electrically insulating oxide. It has a band gap of 3.4 eV and becomes conducting after creating oxygen vacancies [6]. It is possible to accommodate a large concentration of mobile oxygen vacancies by reduction or doping giving rise to high ionic conductivity and a large oxygen storage capacity. As a result, ceria plays an important role as a component in the active noble metal support in automotive three-way catalytic converters, where NO_x , CO, and hydro-carbons are simultaneously removed [1, 7]. Due to other important properties of CeO_2 , such as a high dielectric constant and good epitaxy on Si, it is also viewed as a perspective material for future microelectronic applications. In particular, CeO_2 is considered as a candidate for replacing silicon dioxide in electronic appliances [8].

Although several theoretical and experimental works devoted to cerium dioxide have been already published [9–13], owing to the importance of this material further examination of its structure and properties including electron correlations explicitly is still necessary. Here we present the results obtained by the method of increments [14]. Hartree-Fock (HF) self-consistent field (SCF) calculations performed for the periodic solid are used as a starting point for the systematic inclusion of electron-correlation effects, which are considered by using an expansion of the total correlation energy in terms of one-body, two-body, and higher contributions, the so-called “local increments”. This method has been successfully applied to covalently bound solids such as diamond, graphite and many typical semiconductors [14–19], and to ionic solids, including several oxides (MgO, CaO, NiO) [20–24]. Since ceria contains heavy elements its *ab initio* quantum-chemical study requires the inclusion of relativistic effects. To a great extent, the treatment of such effects can be achieved through the use of effective core potentials (*ecp*) (also called pseudopotentials). In this approach the valence as well as outermost core-electrons are considered explicitly. Inclusion of the outermost core-electrons has a crucial importance for an adequate description of the chemical bond in the systems with rare-earth elements. The relativistic effects are usually treated implicitly.

The paper is organized as follows. The computational methods are outlined in the next

section (Sec. II). Section III is devoted to discussion of the obtained results. In this section thermodynamic, mechanical, and electronic properties of CeO₂ obtained at the HF (Sec. III A) as well as the DFT level of theory (Sec. III B) are shown. Details of the application of the method of increments, individual correlation-energy increments and the influence of correlations on the thermodynamic and mechanical properties of cerium dioxide are discussed in section III C. Our conclusions are summarized in the last section (Sec. IV).

II. METHODS OF CALCULATIONS

For finite systems various *ab initio* program packages based on Gaussian type atomic orbitals (GTOs) are nowadays available for accurate calculation of their properties using a many-body wavefunction ansatz. For solids wavefunction-based HF calculations have become possible with the advent of the program package CRYSTAL [25]. The HF Hamiltonian *a priori* does not include the effects of electron correlation. This leads to an overestimation of the electron-electron repulsion energy and, as a consequence, to a too high total energy. The most widely used method to include correlations in solids is density functional theory (DFT). In principle, DFT models are able to capture the full correlation energy. In practice, present generation methods exhibit a number of serious deficiencies, and wavefunction-based approaches for calculating the correlation energy yield, in contrast, an opportunity of systematically improvable methods. Moreover, for a proper microscopic treatment of electron correlations it is necessary to go beyond the one-particle framework and to deal with many-body wavefunction. Unfortunately, quantum-chemical correlation models are not directly applicable to periodic systems. However, the recently developed method of increments [14] allows an expansion of the bulk correlation energy using information from quantum-chemical calculations on finite clusters. The main ideas of the method are:

- Starting from SCF calculations localized orbitals are generated which are assumed to be similar in the clusters and in the solid (for a detailed study of the validity of this assumption see [26]).
- One-body correlation-energy increments ϵ_A and ϵ_B are calculated, applying any size-extensive correlation method. For that only the electrons of the local orbitals group A and B , respectively, are correlated, whereas the rest is frozen at the HF level.

- Two-body increments are defined as nonadditivity corrections:

$$\Delta\epsilon_{AB} = \epsilon_{AB} - [\epsilon_A + \epsilon_B],$$

where ϵ_{AB} is the correlation energy of the joint orbital system of AB .

- Three-body increments are defined as

$$\Delta\epsilon_{ABC} = \epsilon_{ABC} - [\epsilon_A + \epsilon_B + \epsilon_C] - [\Delta\epsilon_{AB} + \Delta\epsilon_{BC} + \Delta\epsilon_{AC}].$$

where ϵ_{ABC} is the correlation energy of the joint orbital system of ABC . A similar definition can be applied to higher-body increments.

- The correlation energy of the solid can now be expressed as the sum of all possible increments:

$$\epsilon_{\text{bulk}} = \sum_A \epsilon_A + \frac{1}{2!} \sum_{AB} \Delta\epsilon_{AB} + \frac{1}{3!} \sum_{ABC} \Delta\epsilon_{ABC} + \dots$$

Of course, this only makes sense if the incremental expansion is well convergent, i.e. if $\Delta\epsilon_{AB}$ rapidly decreases with increasing distance between the ions at position A and B and if the three-body terms are significantly smaller than the two-body ones.

III. RESULTS AND DISCUSSION

A. Hartree-Fock calculations

A starting point for the treatment of the many-body correlation effects in solids is a reliable HF SCF result for the infinite system. We performed HF ground-state calculations for cerium dioxide, using the program package CRYSTAL98.

The CRYSTAL-code does not allow the inclusion of f -type atomic orbitals into the basis set. The $4f$ -levels of Ce in CeO_2 were assumed unoccupied. Experimental studies on the bulk and surfaces of nearly pure CeO_2 suggest that this approximation is valid for the stoichiometric CeO_2 [27] (but not for systems containing Ce^{3+} , in which the extra electron would be localized on the Ce $4f$ level). Thus, in CRYSTAL-calculations we have used for Ce a pseudopotential derived by Dolg *et al.* for tetravalent cerium ($4f^0$ -subconfiguration, *ecp46*) and the corresponding basis set [28]. For application in the CRYSTAL calculations the basis set has to be modified: very diffuse exponents which are necessary to properly describe

the tails of the free-atom wavefunctions cause numerical problems in CRYSTAL, because of the large overlap with the basis functions of the neighboring atoms in a dense-packed crystal. Therefore, the most diffuse orbitals were optimized by changing the exponents of the Gaussian. The optimization was done in order to minimize the total energy per unit cell while maintaining SCF stability. The resulting exponents (corresponding to the $e^{-\alpha r^2}$ of the GTO) are $\alpha_s=0.10$, $\alpha_p=0.10$, $\alpha_d=0.30$ and 0.19 for s -, p -, and d -functions, respectively. The oxygen basis set employed was 6-31G* [29]. Since the question of Ce $4f$ -occupation in CeO₂ is still under discussion [10, 11, 30, 31], similar calculations have been performed for $4f^1$ -subconfiguration (*ecp47*) of Ce-atom [32] (the corresponding optimized exponents are $\alpha_s=0.10$, $\alpha_p=0.10$, $\alpha_d=0.19$) to find the configuration with the lowest energy.

The experimental value of the cohesive energy ($E_{\text{coh}}^{\text{exp}}$) can be derived by appropriate Born-Haber thermodynamical cycle analysis:

$$E_{\text{coh}}^{\text{exp}} = \Delta H_f - \Delta H_s - D,$$

where ΔH_f is the heat of formation of solid CeO₂ at 298 K (-1089.4 kJ/mol [33]); ΔH_s stands for the heat of sublimation of the metal at 298K (111.6 kcal/mol [34]); and $D = 493.5$ kJ/mol [35] is the dissociation energy of the oxygen molecule. Thus, $E_{\text{coh}}^{\text{exp}}$ is equal to -0.7807 a.u.

On the other hand, the cohesive energy is defined as

$$E_{\text{coh}} = E_{\text{total}} - \sum^N E_a$$

where E_a is the atomic energy for each atom belonging to the crystal unit cell and N is the number of atoms in the unit cell. The choice of an atomic reference energy is a fundamental point in the evaluation of the cohesive energy. As the basis set is not complete, two different basis sets must be used for isolated atoms and for bulk: the same basis set is used for inner electrons, whereas extra functions must be added to the bulk basis set for an accurate description of the valence electron of the isolated atoms. Another possibility to correct the basis set superposition error is to apply the counterpoise method [36]. In our calculations all bulk basis functions of the first as well as the second next neighbors were taken into account via “dummy” atoms, i.e. the corresponding basis set was placed at the position of these atoms, but no nuclear charge or electrons were supplied. The quantum-chemical *ab initio* program system MOLPRO 2002 [37] was used in these calculations.

In Table I the cohesive energies obtained at HF level for f^0 - and f^1 -subconfigurations are presented. It is necessary to note, that for the f^0 case (*ecp46*) we have to consider d^2s^2 -subconfiguration as ground state for the free atom. At the same time, in the case of *ecp47* $4f^1$ state is already included by the pseudopotential. In order to take into account this difference for comparison of cohesive energies obtained in both cases, we performed the atomic calculations for s^2d^2 as well as for $s^2d^1f^1$ configurations of Ce, using the small-core pseudopotential (*ecp28*) [38] and the corresponding basis set [39], increased by even tempered basis functions [40]. As it can be expected the $s^2d^1f^1$ configuration is lower in energy as compared with s^2d^2 . The corresponding energy difference consists of approximately 0.11 a.u. at HF as well as CCSD level. Therefore, for proper comparison with experiment the value of cohesive energy obtained for f^0 -case has to be corrected by this energy difference: $E_{\text{coh}} = -0.5718 + 0.1128 = -0.4590$ a.u. Thus, the HF result obtained for $4f^0$ -Ce is lower in energy than the one obtained for $4f^1$ -Ce.

To calculate the lattice constant and bulk modulus we performed a 4th order polynomial fit to the SCF ground-state energy evaluated from -1 % to +8 % of the experimental lattice parameter (Fig. 2). It is necessary to note here, that the experimental lattice constant available in the literature (5.41 Å [5]) was obtained at room temperature. For better comparison of the calculated lattice parameter with the measured one, experimental lattice constant has to be extrapolated to low temperatures [41]: $a_{T=0\text{K}} \approx 5.40$ Å. The ground-state equilibrium lattice constant a was found to be 5.55 Å at the HF level with f^0 -occupation, that is about 2.5 % higher than the experimental value. This corresponds to a unit cell volume error of ~ 8 %.

The bulk modulus of the cubic structure can be determined according to the formula

$$B = \left(\frac{4}{9a} \frac{\partial^2}{\partial a^2} - \frac{8}{9a^2} \frac{\partial}{\partial a} \right) E(a)$$

where a is the lattice constant. We calculated the bulk moduli at $a = 5.55$ Å and at the experimental one. The bulk modulus at the HF lattice constant is in a good agreement with experimental value. The HF bulk modulus calculated at the experimental lattice constant (307 GPa) is by 30 % higher than the measured one (236 GPa [42]) (Tab. I).

The lattice constant obtained from the minimum of the polynomial fit in the case of f^1 -Ce is much too large (by 8.2 %) compared with the experimental value. The bulk modulus, calculated at the experimental lattice constant, is much too small, only 58 % of the measured

one. It is only slightly changing with increasing lattice constant up to the calculated value. So, we can conclude, that *ecp47* can probably not describe the bulk modulus of CeO_2 . The result supports the tetravalent Ce in cerium dioxide.

The HF-calculated electronic band structures of CeO_2 with cerium in f^0 - as well as f^1 -configuration are presented in Fig. 3a,b. Since CRYSTAL-code does not allow the inclusion of f -type atomic orbitals into the basis set, the Ce $4f$ bands, which are the lowest unoccupied levels in the solid, are not presented in the calculated band structures. Nevertheless, one can see the electronic density unequal to zero in the case of f^1 -Ce as opposite to the insulating f^0 -case.

The energy gap between the occupied $2p$ band of O and unoccupied band of $5d$ states of Ce is about 11.4 eV and 13.8 eV for CeO_2 with f^1 - and f^0 -subconfiguration of cerium atom, respectively, i.e. there is an overestimation of this energy difference ($\Delta E_{\text{exp}}=6$ eV [27, 43]), that is typical for the HF Hamiltonian.

B. DFT calculations

In order to estimate the influence of correlations the so-called *a posteriori*-HF correlation DFT method was applied to calculate the ground-state properties of cerium dioxide. In this scheme the total energies of cerium dioxide (with CRYSTAL98) as well as atomic energies (with MOLPRO2002) are expressed by the summation of the HF energy and the corresponding correlation energy which was evaluated for PW-LSD [44] and PW-GGA [45] correlation functionals in conjugation with exact Hartree-Fock exchange. The obtained values are summed in Tab. I. For the correlation contribution to the cohesive energy ($E_{\text{coh}}^{\text{exp}} - E_{\text{coh}}^{\text{HF}}$) we recover 22 % and 37 % with the PW-LSD and the PW-GGA functionals, respectively. The trends are in the right direction, but the magnitude obtained with post-HF DFT treatments is too small. The lattice constant is shifted to smaller values, for PW-GGA it agrees well with experiment.

Further, a full potential nonorthogonal local-orbital scheme (FPLO) [46] within the local density approximation (LDA) was used to obtain the total energies and accurate band structure. In the full relativistic calculations we used the exchange and correlation potentials of Perdew and Wang [44]. Ce $5s, 5p, 6s, 5d, 4f, 6p$ and O $2s, 2p, 3d$ states were chosen as the basis set. The lower-lying Ce and O $1s$ states were treated as core states. The O $3d$ and

Ce $6p$ states were taken into account to get a more complete basis set. The inclusion of the Ce $5s$ and $5p$ in the valence states was necessary in order to handle non-negligible core-core overlaps. The spatial extension of the basis orbitals, controlled by a confining potential $(r/r_0)^4$ [47], was optimized to minimize the total energy. A \mathbf{k} mesh of $24 \times 24 \times 24$ in the Brillouin zone was used. The atomic energies used in the calculation of cohesive energy presented in Tab. I were obtained with DIRAC-code [48]. One can see (Tab. I) that the lattice parameter and the bulk modulus as well as the cohesive energy obtained within this approach are in good agreement with the experiment.

Performing a DFT-LDA calculation with CRYSTAL-code (PW-LSD for correlation and Dirac-Slater exchange functional (LDA) [49]) we obtain a cohesive energy of -0.81037 a.u., that is in good agreement with the FPLO-LDA as well as with experiment. At the same time it becomes clear after comparison of this value with the one obtained with post-HF LDA, that the good agreement with the experiment is due to an error cancelation: the LDA exchange overestimates the cohesive energy and the LDA correlation term underestimates it.

Fig. 3c shows the electronic band structure of CeO_2 calculated with FPLO-code. In this figure the lowest shown band consists of $5p$ states of Ce. The highest occupied valence band has mostly O $2p$ character, while the narrow band situated just above the Fermi level is mainly due to $4f$ states of Ce (marked by dashed frame in Fig. 3c). The energy gap between the $2p$ O band and unoccupied $4f$ Ce band is about 2.3 eV which is little low than the experimental value (3.4 eV [27, 43]): the usual underestimation of the band gap within the standard LDA scheme. The energy difference between the occupied $2p$ band of O and unoccupied $5d$ Ce band is about 6.2 eV, which agrees well with measurements ($\Delta E_{\text{exp}} = 6$ eV [27, 43]). According to the calculations CeO_2 is an insulator, that is also in agreement with experiment as well as the HF/*ecp46*-calculation result. This observation, along with analysis of mechanical and thermodynamic values calculated for both electronic subconfigurations of Ce, allows us to conclude that the f^0 -configuration of cerium atom in CeO_2 is more favorable.

C. Application of the method of increments

1. Embedding procedure

Since dynamic correlations have local character (and, as a consequence, the increments are fairly local entities), the increments can be calculated in finite fragments of the solid. Therefore, an appropriate embedding procedure simulating the influence of the infinite system surrounding the chosen cluster is of crucial importance. Since in the studied system valence electrons are located at the oxygen we selected for the calculations the O-centered cluster Ce_4O_7 : the central O-ion with four neighboring ceriums according to the crystal structure and 6 additional O-ions connecting the ceriums by pairs (Fig. 4). For Ce we used the *ecp46* and the corresponding basis set $((7s6p5d2f)/[5s4p3d2f])$ increased by even tempered basis functions to $[8s7p6d3f2g]$ [50]. Oxygen was treated with the augmented valence triple- ζ (*avtz*) basis set by Dunning [51]. An additional cover consisting of twelve Ce^{4+} describing by large-core potential (*ecp54*) together with a contracted $[1s1p1d1f]$ basis set [52] were added as shown in Fig. 4. The obtained structure is further surrounded by a point-charge area which simulates the $2 \times 2 \times 2$ unit cell construction (larger point charge array would yield nearly no changes in the values of correlation increments). The correlation energies are evaluated using the coupled cluster approach with single and double excitations (CCSD) [53] as implemented in MOLPRO 2002. Localized orbitals used in these calculations were obtained according to the Pipek-Mezey criterion [54]. The results for the one- and two-body increments are shown in Table II. The presented embedding approach has several advantages. At first, the cluster describes the proper surrounding of the valence electrons of the correlated oxygen. This leads to the assumption, that the increments obtained from this cluster are very close to the ones in the solid. Then, there is a possibility to get a large number of increments from the same cluster. At the same time, as can be seen from Tab. II, the studied cluster allows to consider only finite number of increments. The idea to use CeO_8 -cluster in order to find $\Delta\epsilon_{\text{O}-(\text{Ce})-\text{O}}$ was faulty because of the instability of this highly negatively charged cluster. The correlation-energy increments $\Delta\epsilon_{\text{O}-(\cdot)-\text{O}}$ as well as $\Delta\epsilon_{\text{Ce}-\text{Ce}}$ with $r_{\text{Ce}-\text{Ce}} = 5.41 \text{ \AA}$ could be evaluated from the cluster, which is the “sum” of two Ce_4O_7 - clusters [55], but these calculations will require a significant amount of computational resources. Besides that we can not consider some Ce-O and Ce-Ce increments

with the distance between the centers larger than the lattice parameter ($a=5.41 \text{ \AA}$) with the investigated cluster. For these reasons we decided to use also the alternative embedding scheme, where each particular increment can be obtained from an individual cluster. This approach was shown to work well for several ionic compounds [20–22, 24]. In this scheme the individual ions can be embedded in different ways. We have tested several embeddings: from purely point charges up to pseudopotential-surrounding of oxygens to imitate the Ce-ions [26]. The results shown here (*see* Tab. II) were obtained for the case, where correlated negatively charged ions are embedded with Ce^{4+} -pseudopotentials (*ecp46*) as next neighbors. 8 outer-core electrons of the embedding-ceriums in the $5s^2p^6$ shell are described with a minimal basis set. The *avtz* and $[8s7p6d3f2g]$ basis sets are used for the correlated O and Ce, respectively, as in the previous calculations. Finally, the system is surrounded by a set of point charges in accordance with the crystal symmetry.

2. One-body increments

One can see from Tab. II the value obtained for the Ce-increment with the second approach is by 0.0063 a.u. lower as compared with the first one, whereas in the case of ϵ_{O} calculated with the second approach we obtained a value which is by 0.0036 a.u. higher than the one obtained with the first embedding-scheme. Nevertheless, summation of the one-body increments multiplied with their respective weight factors leads to the nearly identical correlation contribution (of -0.69728 a.u. or -0.69646 a.u. in the case of the first and the second embedding-scheme, respectively) to the total energy of cerium dioxide. This value corresponds to approximately -0.1210 a.u. contribution to the bulk cohesive energy E_{coh} per primitive unit cell of the CeO_2 -crystal or yields to $\sim 58\%$ of the “experimental” correlation contribution to the cohesive energy, i.e. the difference between $E_{\text{coh}}^{\text{exp}}$ and the HF cohesive energy.

3. Two- and three-body increments

Among the two-body increments let us first discuss the interaction of ions with the opposite signs. In this series we examined Ce-O correlation-energy increments up to the third nearest neighbor Ce and O ($r_{\text{Ce-O}} \leq 6 \text{ \AA}$). Whereas the interaction between the nearest

neighbor Ce^{4+} and O^{2-} leads to the largest contribution among all two-body increments, the Ce-O correlation-contributions between second and third next neighbor ions are found to be relatively small, but can not be neglected due to their high weight factor (24).

The sum of increments related to the pairs of Ce^{4+} -ions (-0.0062 a.u.), amounts to only 3% of the total sum of two-body increments. More important are interactions between O^{2-} -ions. The 6 calculated increments of this kind (*see* Tab. II) up to $r_{\text{O-O}} = 6.05 \text{ \AA}$ decrease quite quickly with increase of interionic distance. The sum of $\Delta\epsilon_{\text{O-O}}$ contribute about 17% to the sum of two-body increments.

We have calculated 11 different three-body increments. As can be clearly seen from Tab. III they are very small: they contribute less than 1% to the correlation part of the bulk cohesive energy. This indicates a rapid convergence of the incremental expansion. Therefore, we can conclude that neglecting three-body increments in further calculations is a reasonable approximation.

4. Sum of increments and discussion

Adding up the increments we obtain about 85% of the experimental cohesive energy. In order to improve this result we expand the basis set at Ce and O up to $[9s8p7d4f3g1h]$ [56] and $avqz$ [51], respectively. On the other hand it is interesting to study also the influence of triple excitations to the incremental expansion. The data obtained for the improved basis set at the CCSD level, as well as coupled cluster level with single and double excitations augmented by a perturbative correction for connected triple excitations [CCSD(T)] [57], are presented in Tab. II.

One can see, that increasing the basis set as well as including triple excitations in the CC expansion have a rather high influence on the total sum of increments and their contribution to the cohesive energy. Turning to the values of individual increments, one can note, that the listed changes play a far more important role for the oxygen one-body increment (ϵ_{O}) as compared with the one for cerium. In the case of ϵ_{O} we get +9% due to the use of $avqz$ instead of $avtz$ and another +3% as a result of triples' contribution. At the same time for ϵ_{Ce} this corresponds to +3.5% and +2.5%, respectively. Among the two-body increments $\Delta\epsilon_{\text{O-O}}$ are most exposed to the effects of changes in the basis set and CC model: increments obtained at CCSD level with $avqz$ are by about 20% higher than the ones obtained with

avtz basis set. Application of CCSD(T) model leads to increase of this value by another 16%. For the rest the general behavior of the increments are similar when compared with the ones obtained as described in Sec. III C 3.

Thus, using the [9s8p7d4f3g1h] and *avqz* basis sets for cerium and oxygen, respectively, at the CCSD(T) level of theory we can cover nearly 93% of the expected cohesive energy (see Tab. I). A basis set extrapolation at the correlated level [58] would yield an increase of the cohesive energy by about 1%. But also the basis set limit is probably not reached at the HF level, so we can expect an increase of the HF cohesive energy by 1-2%. Errors due to truncation of the incremental expansion can be estimated to about $\pm 3\%$. Note, that according to Harrison [59], the experimental error of the cohesive energy, due to measuring the heat of formation and the heat of atomization at different temperatures, is about 1%. At the same time the best DFT results (FPLO) overestimate the cohesive energy by approximately 9%.

5. Mechanical properties

At the HF level the lattice constant has a deviation of 0.14 Å from the experimental value. It is interesting, therefore, to study the influence of correlation effects on lattice parameter.

Application of the CCSD(T) model together with the “good” basis set requires significant computational resources even within the second embedding approach. At the same time it is necessary to note here, that the calculated lattice constant and bulk modulus are strongly influenced by the form of the potential curve and we do not expect significant dependence of the calculated mechanical properties on the type of the CC model and quality of the used basis set. Therefore, for the optimization of the lattice constant we decided to use the *avtz* and [8s7p6d3f2g] basis sets for the correlated O and Ce, respectively, at the CCSD level of theory. Summing up one and two-body correlation contributions, the lattice constant was found to be 5.43 Å, i.e. about 0.4% larger than the measured parameter (see Fig. 5a). The bulk modulus, obtained for the calculated lattice constant (240 GPa) is about 2% higher than the experimental value. The bulk modulus calculated at the experimental lattice constant (255 GPa), is by 8% too large compared to the measured one. To obtain these results we applied a quadratic fit to the correlation energy and 4th order polynomial fit to the HF potential curve.

As was already found for previously studied systems [20–22], there are two main effects of the correlations. On the one hand, the one-body increments enforce a larger lattice constant (see Fig 5b, closed circles), due to the increasing of the quantum well enclosing the oxygen ion which leads to the lower excitation energies. It is evident, at the same time, that since in Ce^{4+} only outer-core electrons are correlated, ϵ_{Ce} is weakly influenced by lattice parameter. On the other hand, the two-body increments yield a large reduction of the lattice constant (see Fig. 5b, triangles). Due to the inclusion of correlations the electrons can “avoid each other” better and therefore a shorter interatomic distances is favourable.

IV. CONCLUSION

The electron-correlation effects on the ground-state properties of the cerium dioxide were studied by *ab initio* quantum-chemical methods. First, the cohesive energy, lattice constant and bulk modulus of the cerium dioxide were determined at the HF level. With this method we recover about 60% of the experimental cohesive energy. The lattice constant is overestimated by 2.5% and bulk modulus, evaluated at the experimental lattice constant is too large. Then, the correlation contribution to the ground-state properties of CeO_2 was calculated using an expansion into local increments. After inclusion of correlations obtained at the CCSD(T) level the calculated values are in good agreement with experiment: we obtained about 93% with an estimated error of $\pm 4\%$ of the expected cohesive energy. The computed lattice constant shows a deviation of less than 1% from the experimental one. The calculated bulk modulus overestimates the measured value by 8%. With this detailed description of the electronic correlations in bulk CeO_2 it is now possible to extend the work to CeO_2 surfaces and adsorbed molecules on it.

Acknowledgments

We thank Prof. Dr. P. Fulde (Dresden) and Prof. Dr. H. Stoll (Stuttgart) for many valuable discussions and C. Müller (Uppsala) for drawing our attention to this problem.

[1] A. Trovarelli, Catal. Rev. - Sci. Eng. **38**, 439 (1996).

- [2] W. J. Coleman, *Appl. Opt.* **13**, 946 (1974).
- [3] K. B. Sundaram, P. F. Wahid, and P. J. Sisk, *Thin Solid Films* **221**, 13 (1992).
- [4] H.-J. Beie and A. Gnich, *Sensors and Actuators B* **4**, 393 (1991).
- [5] R. W. G. Wyckoff, *Crystal Structures*, 2nd ed. (Interscience, New York, 1963).
- [6] C. Binet, A. Badri, and J.C. Lavalley, *J. Phys. Chem.* **98**, 6392 (1994); A. Holmgren and B. Andersson, *J. Catal.* **178**, 14 (1998); L. Minervini, M. O. Zacate, and R. W. Grimes, *Solid State Ionics* **116**, 339 (1999); A. Pfau and K. D. Schierbaum, *Surf. Sci.* **71**, 321 (1994).
- [7] K. C. Taylor, *Catal. Rev. - Sci. Eng.* **35**, 457 (1993); J. Kaspar, P. Fornasiero, and M. Graziani, *Catal. Today* **50**, 285 (1999).
- [8] T. Nakazawa, T. Inoue, M. Satoh, and Y. Yamamoto, *Jpn. J. Appl. Phys., Part 1* **34**, 548 (1995).
- [9] S. Gennard, F. Cora, and C. R. A. Catlow, *J. Phys. Chem. B* **103**, 10158 (1999); S. E. Hill and C. R. A. Catlow, *J. Phys. Chem. Solids* **54**, 411 (1993).
- [10] F. Goubin, X. Rocquefelte, M.-H. Whangbo, Y. Montardi, R. Brec, and S. Jobic, *Chem. Mater.* **16**, 622 (2004).
- [11] Z. Yang, T. K. Woo, M. Baudin, and K. Hermansson, *J. Chem. Phys.* **120**, 7741 (2004).
- [12] A. Fujimori, *Phys. Rev. B* **27**, 3992 (1983).
- [13] N. V. Skorodumova, R. Ahuja, S. I. Simak, I. A. Abrikosov, B. Johansson, and I. Lundqvist, *Phys. Rev. B* **64**, 115108 (2001).
- [14] H. Stoll, *Phys. Rev. B.* **46**, 6700 (1992).
- [15] H. Stoll, *Chem. Phys. Lett.* **191** 548 (1992).
- [16] H. Stoll, *J. Chem. Phys.* **97** 8449 (1992).
- [17] B. Paulus, F.-J. Shi, and H. Stoll, *J. Phys.: Cond. Matter* **9**, 2745 (1997).
- [18] B. Paulus, P. Fulde, and H. Stoll, *Phys. Rev. B* **54**, 2556 (1996).
- [19] S. Kalvoda, B. Paulus, P. Fulde, and H. Stoll, *Phys. Rev. B* **55**, 4027 (1997).
- [20] K. Doll and H. Stoll, *Phys. Rev. B* **56**, 10121 (1997).
- [21] K. Doll, M. Dolg, P. Fulde, and H. Stoll, *Phys. Rev. B* **52**, 4842 (1995).
- [22] K. Doll, M. Dolg, and H. Stoll, *Phys. Rev. B* **54**, 13529 (1996).
- [23] K. Doll, M. Dolg, P. Fulde, and H. Stoll, *Phys. Rev. B* **55**, 10282 (1997).
- [24] S. Kalvoda, M. Dolg, H. J. Flad, P. Fulde, and H. Stoll, *Phys. Rev. B* **57**, 2127 (1998).
- [25] C. Pisani, R. Dovesi, and C. Roetti, in: *Lecture Notes in Chemistry: Hartree-Fock Ab Initio*

- Treatment of Crystalline Systems*, edited by G. Berthier *et al.*, Vol. 48 (Springer, Berlin, 1988).
- [26] E. Voloshina and B. Paulus, accepted for the publication in *Theor. Chem. Acc.* (2005).
- [27] E. Wuilloud, B. Delley, W.-D. Schneider, and Y. Baer, *Phys. Rev. Lett.* **53**, 202 (1984).
- [28] M. Dolg, P. Fulde, W. Küchle, C.-S. Neumann, and H. Stoll, *J. Chem. Phys.* **94**, 3011 (1991).
- [29] <http://www.cse.clrc.ac.uk/qcg/basis/>.
- [30] F. L. Normand, J. E. Fallah, L. Hiliare, P. Legare, A. Kotani, and J. C. Parlebas, *Solid State Commun.* **71**, 885 (1989).
- [31] D. D. Koelling, A. M. Boring, and J. H. Wood, *Solid State Commun.* **47**, 227 (1983).
- [32] M. Dolg, H. Stoll, A. Savin, and H. Preuss, *Theor. Chim. Acta* **75**, 173 (1989).
- [33] *CRC Handbook of Chemistry and Physics*, 68th ed., edited by R. C. Weast *et al.* (CRC Press, Florida, 1987).
- [34] C. E. Habermann and A. H. Daane, *J. Chem. Phys.* **41**, 2818 (1964).
- [35] *Handbook of Spectroscopy*, edited by J. W. Robinson, Vol. 1 (CRC, Cleveland, 1974).
- [36] S. F. Boys and F. Bernardi, *Mol. Phys.* **19**, 553 (1970).
- [37] MOLPRO is a package of ab initio programs written by H. J. Werner and P. J. Knowles, with contribution from J. Almlöf, R. D. Amos, M. J. O. Deegan, F. Eckert, S. T. Elbert, C. Hampel, W. Meyer, A. Nicklass, K. Peterson, R. M. Pitzer, A. J. Stone, P. R. Taylor, M. E. Mura, P. Pulay, M. Schuetz, H. Stoll, T. Thorsteinsson, and D. L. Cooper.
- [38] M. Dolg, H. Stoll, and H. Preuss, *J. Chem. Phys.* **90**, 1730 (1989).
- [39] X. Cao and M. Dolg, *J. Chem. Phys.* **115**, 7348 (2001); *cf.* also X. Cao and M. Dolg, *J. Molec. Struct. (Theochem)* **581**, 139 (2002).
- [40] We added two s , p , d , f , and g ($\alpha_s=0.008745$ and 0.003694 , $\alpha_p=0.027766$ and 0.009637 , $\alpha_d=0.03254$ and 0.01026 , $\alpha_f=0.03254$ and 0.01026 , $\alpha_g=0.073584$ and 0.025021 , respectively) exponents and one h exponent (3.06).
- [41] Experimental lattice constant can be extrapolated to low temperatures in accordance to the formula: $\Delta a/a_0 = \alpha \Delta T$, where $\Delta a/a_0$ is the fractional change in lattice constant; α is an expansion coefficient ($\alpha_{\text{CeO}_2} = 7.45 \cdot 10^{-6} \text{ K}^{-1}$ [www.jubochina.com/ceo2.html]); ΔT is the change in temperature.
- [42] L. Gerwald and A. S. Staun-Olsen, *Powder Diffr.* **8**, 127 (1993).
- [43] M. Marabelli and P. Wachter, *Phys. Rev. B* **36**, 1238 (1987).
- [44] J. P. Perdew and Y. Wang, *Phys. Rev. B* **45**, 13244 (1992).

- [45] J. P. Perdew, J. A. Chevary, S. H. Vosko, K. A. Jackson, M. R. Pederson, D. J. Singh, and C. Fiolhais, *Phys. Rev. B* **46**, 6671 (1992).
- [46] K. Koepnik and H. Eschrig, *Phys. Rev. B*, **59**, 1743 (1999).
- [47] H. Eschrig, *Optimized LCAO Method und the Electronic Structure of Extended Systems* (Springer, Berlin, 1989).
- [48] Full-relativistic atom program (version 5), written by K. Köpnerik (2001).
- [49] P. A. M. Dirac, *Proc. Cambridge Phil. Soc.* **26**, 376 (1930).
- [50] We added one s , p , d and f ($\alpha_s=0.010920$, $\alpha_p=0.012178$, $\alpha_d=0.027009$, $\alpha_f=0.103158$, respectively) exponents and two g exponents (0.82 and 0.34).
- [51] T. H. Dunning (Jr), *J. Chem. Phys.* **98**, 1007 (1998); R. A. Kendall, T. H. Dunning (Jr), and R. J. Harrison, *J. Chem. Phys.* **96**, 6796 (1992).
- [52] R. B. Ross, S. Gayen, and W. C. Ermler, *J. Chem. Phys.* **100**, 8145 (1994).
- [53] R. C. Bartlett, *J. Phys. Chem.* **93**, 1697 (1989); J. Paldus, in *Methods in Computational Physics*, edited by S. Wilson and G. H. F. Dierksen (Plenum Press, New York, 1992).
- [54] J. Pipek and P. G. Mezey, *J. Chem. Phys.* **90**, 4916 (1989).
- [55] Two central oxygens at $(a/4, a/4, a/4)$ and $(-a/4, -a/4, -a/4)$, respectively, each surrounded by four Ce^{4+} . This structure has an environment consisting of 12 oxygens and 18 Ce-ions.
- [56] We added two s , p , d and f ($\alpha_s=0.010920$ and 0.004474 , $\alpha_p=0.012178$ and 0.004206 , $\alpha_d=0.027009$ and 0.009277 , $\alpha_f=0.103158$ and 0.038006 , respectively) exponents, three g exponents (0.82, 0.34, and 0.14), and one h exponent (0.93).
- [57] J. Noga and R. J. Barlett, *J. Chem. Phys.* **86**, 7041 (1987); **89**, 3401 (1988); G. E. Scuseria and H. F. Schaefer III, *Chem. Phys. Lett.* **152**, 382 (1988); K. Raghavarchari, G. W. Trucks, J. A. Pople, and M. Head-Gordon, *Chem. Phys. Lett.* **157**, 479 (1989).
- [58] T. Helgaker, W. Klopper, H. Koch, and J. Noga, *J. Chem. Phys.* **106**, 9639 (1997).
- [59] W. A. Harrison, *Electronic structure and the properties of solids* (Dover Publications, Inc., New York, 1989).

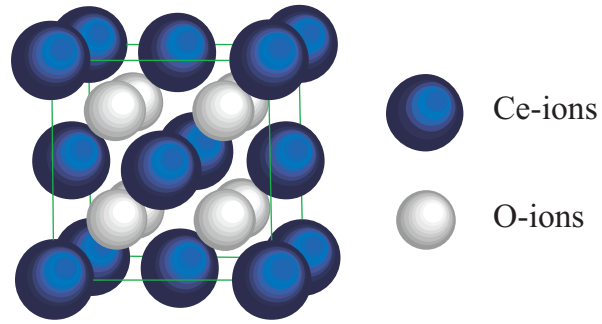


FIG. 1: (Color online) Cubic fluorite structure of cerium dioxide

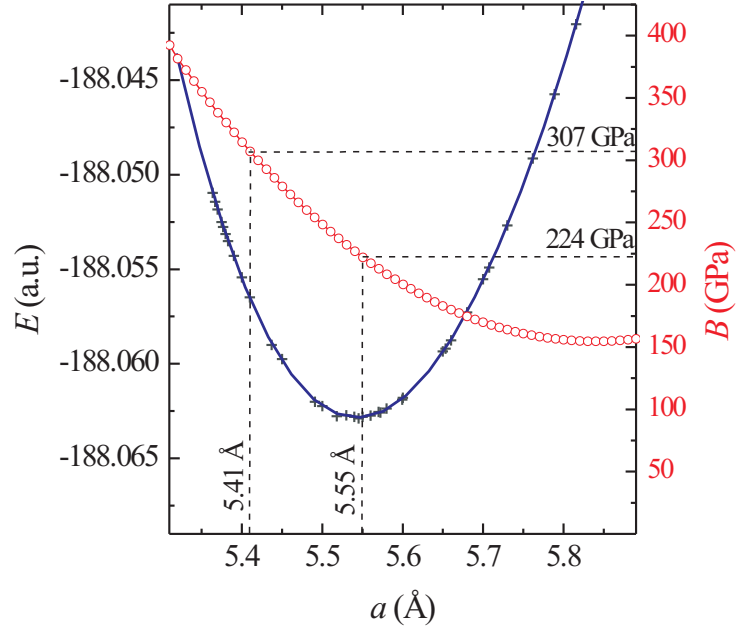


FIG. 2: (Color online) The total energy per unit cell as a function of the lattice parameter a . The crosses are the data-points obtained from CRYSTAL calculations (f^0 -subconfiguration of Ce). Solid line is the fourth-order polynomial fit. Open-circled line is the bulk modulus as a function of the lattice constant a .

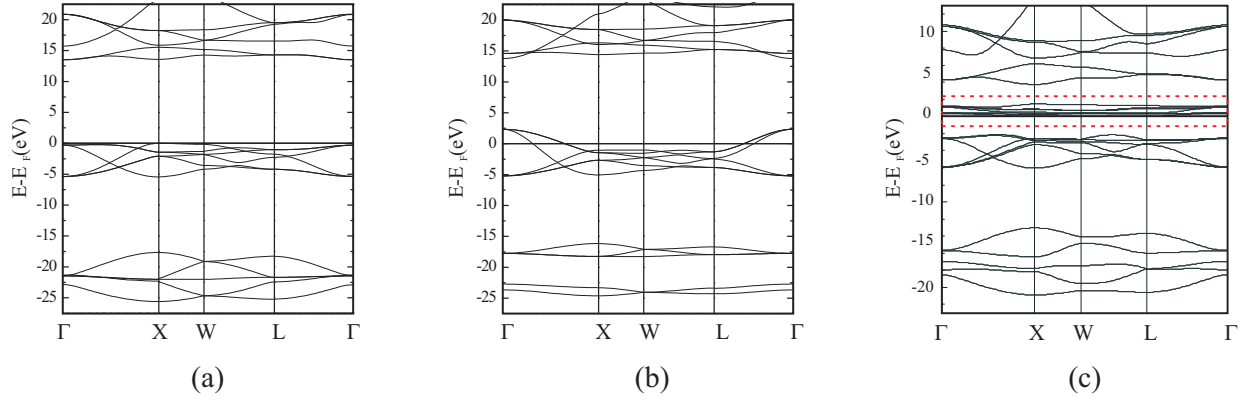


FIG. 3: (Color online) (a) HF-band structure of CeO₂ (f^0 -subconfiguration) shows that CeO₂ is an insulator; (b) HF-band structure of CeO₂ (f^1 -subconfiguration): CeO₂ is a conductor; (c) DFT(FPLO)-band structure of CeO₂ (f -bands are marked by the dashed frame).

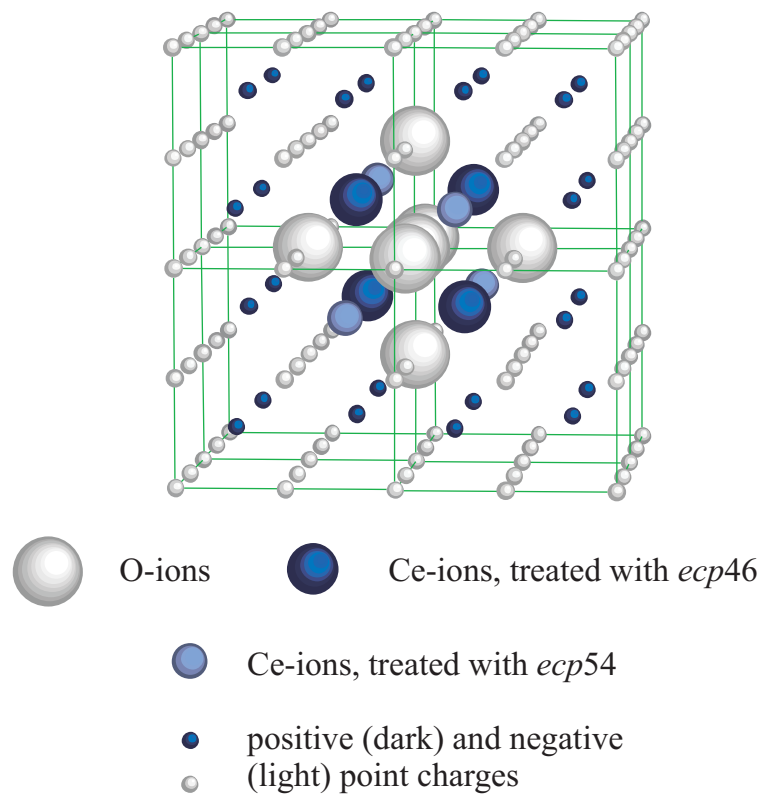


FIG. 4: (Color online) Embedding of the Ce_4O_7 -cluster.

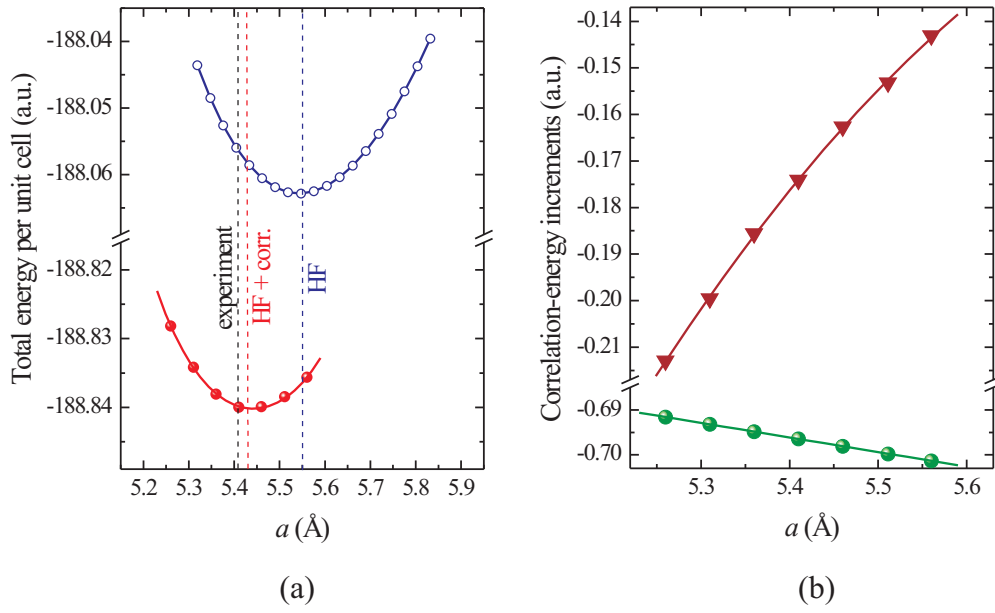


FIG. 5: (Color online) (a) The total energy per unit cell as a function of the lattice constant. The opened cycles are the data obtained at the HF level; closed circles are the ones improved by inclusion of the one- and two-body correlation-energy increments. Dashed lines indicate the experimental lattice constant ($a^{\text{exp}} = 5.41$ Å) as well as the calculated ones ($a^{\text{HF}} = 5.55$ Å and $a^{\text{HF+corr}} = 5.43$ Å) (b) Sum of the one- (closed circles) and two-body increments (triangles) as functions of the lattice constant.

TABLE I: Experimental and calculated lattice constant (a), bulk modulus (B) and cohesive energy (E_{coh}) of CeO_2 .

Exchange	Experi-	HF	HF	HF	HF	LDA ^a	HF
Correlation	ment	–	–	PW-LSD	PW-GGA	LDA ^a	CCSD
PP		<i>ecp46</i>	<i>ecp47</i>	<i>ecp46</i>	<i>ecp46</i>	all-el.	<i>ecp46</i>
a (Å)	5.41 [5]	5.55	5.85	5.47	5.42	5.42	5.43
B (GPa)	236 [42]	307 ^b	139 ^b	298 ^b	272	217	255 ^b
E_{coh} (a.u.)	-0.7807	-0.4590	-0.2091	-0.5298	-0.5778	-0.8524	-0.7266 ^c

^a FPLO-calculations

^b calculated for experimental lattice parameter

^cobtained at CCSD(T) level of theory

TABLE II: Correlation energy increments for CeO₂

Atom (group)	Dist. (Å)	ω^a	ϵ (a.u.) ^b (CCSD, Basis A ^d)	ϵ (a.u.) ^c (CCSD, Basis A)	ϵ (a.u.) ^c (CCSD, Basis B ^e)	ϵ (a.u.) ^c (CCSD(T), Basis B)
One-body increments (ϵ_A)						
Ce	-	1	-0.17418	-0.18048	-0.18654	-0.19080
O	-	2	-0.26155	-0.25799	-0.28052	-0.28942
$\Sigma\epsilon_A$			-0.69728	-0.69646	-0.74758	-0.76964
Two-body increments ($\Delta\epsilon_{AB}$)						
Ce-O	2.34	8	-0.01198	-0.01492	-0.01578	-0.01767
Ce-O	4.49	24	-0.00093	-0.00070	-0.00082	-0.00093
Ce-O	5.90	24		-0.00008	-0.00010	-0.00011
Ce-Ce	3.83	6	-0.00068	-0.00095	-0.00095	-0.00104
Ce-Ce	5.41	3		-0.00016	-0.00016	-0.00017
O-O	2.71	6	-0.00691	-0.00337	-0.00404	-0.00469
O-O	3.83	12	-0.00146	-0.00049	-0.00065	-0.00075
O-(Ce)-O	4.69	4		-0.00044	-0.00048	-0.00057
O-(.)-O	4.69	4		-0.00022	-0.00029	-0.00035
O-O	5.41	6	-0.00021	-0.00010	-0.00012	-0.00014
O-O	6.05	24		-0.00002	-0.00003	-0.00003
$\Sigma\Delta\epsilon_{AB}$			-0.18248	-0.17408	-0.19106	-0.21545

^aweight factor per unit cell

^bobtained from calculations performed for the single cluster (see Fig. 4)

^cobtained from different cluster-calculations

^d[*8s7p6d3f2g*] and *avtz* basis sets for cerium and oxygen were used

^e[*9s8p7d4f3g1h*] and *avqz* basis sets for cerium and oxygen were used

TABLE III: Three-body correlation-energy increments determined at the CCSD level.

	Distances (\AA)			ω	ϵ^a (a.u.)
Ce-Ce-Ce	3.83	3.83	3.83	4	-0.000008
Ce-Ce-O	3.83	2.34	2.34	8/3	-0.001249
Ce-Ce-O	3.83	2.34	4.49	8/3	-0.000312
Ce-Ce-O	3.83	4.49	4.49	4/3	+0.000042
Ce-O-O	2.34	2.71	2.34	5/3	-0.000157
Ce-O-O	2.34	2.71	4.49	40/9	+0.000056
Ce-O-O	2.34	5.41	4.49	5	+0.000636
O-O-O	2.71	3.83	2.71	8	-0.000128
O-O-O	3.83	3.83	3.83	16	-0.000155
O-O-O	2.71	5.41	2.71	2	-0.000091
O-O-O	3.83	5.41	3.83	44/3	+0.000288
$\Sigma\Delta\epsilon_{ABC}$					-0.000433

^a obtained from different cluster-calculations